A STATISTICAL APPROACH TO MOTION COMPENSATED CONE-BEAM RECONSTRUCTION

Mark Lyksborg , Mads Fogtmann Hansen, Rasmus Larsen

Technical University of Denmark,
Informatics and Mathematical Modelling,
Richard Petersens Plads, Building 321, DK-2800 Kgs. Lyngby, Denmark

ABSTRACT

One of the problems arising in radiotherapy planning is the quality of CT planning data. In the following attention is giving to the cone-beam scanning geometry where reconstruction of a 3D volume based on 2D projections, using the classic Feldkamp-Davis-Kress (FDK) algorithm requires a large number of projections to be adequate. Since the patients are breathing freely during a scan, the number of projections with similar respiration may be to low. In the following we use an iterative reconstruction combined with the simultaneous estimation of the motion field, to improve reconstruction in these situations. Using a simulated dataset we demonstrate that this combination outperforms the FDK but due to ill possessedness of the motion estimation it is only on par with the sole iterative method.

Index Terms— Image reconstruction, Image registration, Motion modelling, Cone-beam, Optimization

1. INTRODUCTION

The Feldkamp-Davis-Kress algorithm [1] remains the method of choice for 3D CT reconstruction from 2D cone-beam projections due to its highly efficient implementation. The problem with the FDK algorithm is the degradation of the reconstructions when the numbers of projections decrease.

Using all projections from a scan rotation, for imaging of the thorax region, yields enough projections for reconstruction but will result in blurred reconstructions caused by respiration motion. A classic solution is to sort the projections according to respiratory phase and reconstruct several volumes with limited motion artefacts based on fewer projections.

In recent years people have attempted to model the respiration motion of the patient [2], and others have attempted to include this into the reconstruction framework. For instance [3] and [4], both estimate the 4D motion model from the CT planning data and include this into the FDK algorithm, allowing for motion correction and usage of all projection data. As the authors note such a model is problematic since patients breathing patterns may change over time. This observation promotes the idea of learning the motion model from the 2D projections. The approach of estimating motion and reconstructing was recently investigated in [5] by Zhang et al. who used it to reconstruct the vascular heart morphology with a mutual information similarity measure. Prior to this work Zeng et al. had suggested in [6] how to estimate the motion from the projections. They examined the different image similarity metrics of sums of squared differences and image cross correlation.

Like in [6] we estimate the motion but do not assume a static CT prior which is forward projected in order to estimate motion. Instead we attempt to reconstruct both the volume and motion simultaneously. This is achieved using a maximum likelihood cost function for the simultaneous estimation of motion and attenuation coefficients. An L-BFGS-B optimizer [7] is used to iteratively fit the attenuation parameters as well as the deformable model parameters.

We investigate how the reconstruction of cone-beam CT benefits from the simultaneous estimation of a motion model and compare this to the phase sorted iterative reconstruction. Furthermore these reconstructions are compared to a basic implementation of the phase sorted FDK approach [1]. Including motion into the iterative reconstruction framework shows promising results.

2. THE CONE-BEAM GEOMETRY AND MODEL

Knowledge of the x-ray geometry is essential to the reconstruction problem. Cone-beam projections are acquired by emitting x-rays from a point source towards a 2D detector plate consisting of smaller sensor pixels, which measures the dampened x-rays. The source and detector rotates while acquiring projection images at different angular positions. Using the knowledge of the rotation angles, the source to axis distance (SAD) and the source to detector distance (SDD), it is possible to calculate the x-ray lines trajectory and reconstruct the attenuation of the subject. The expected number of recorded photons [8] by the ith sensor is given by

$$E[P_i] = c_i \cdot e^{-\int_{L_i(\varphi)} \mu(\vec{x}) \partial \vec{x}} + r_i, \qquad (1)$$

where $E[P_i]$ is the estimate given by the forward projection model and the r_i component is system depend noise and since we are working with simulated data we can assume this to be zero. The c_i parameter is a detector depend parameter of the ith sensor.

3. METHOD

We reconstruct an attenuation volume and possible motion field by solving

$$\max_{\varphi,\mu} C = \sum_i d(p_i, E[P_i]), \tag{2}$$

where we are looking for the attenuation volume μ and the deformation φ that optimises the criteria d. When deformation is neglected the projection model is evaluated by integrating along a straight line L_i from the x-ray source to the ith sensor and exponentiating. Inclusion of deformation allows to use projections from all respiratory phases in the reconstruction of each individual phase. In practice using deformation corresponds to integrating along curves, denoted $L_i(\varphi)$. Throughout the subsections 3.1-3.4, specific choices of μ, φ, d are given and the optimization scheme for solving Eq.(2) is presented.

3.1. The image attenuation model

The simplest way of representing attenuation is with a voxel based grid. A model that is better suited than a simple voxel representation is the spline function $\mu : \Re^3 \rightarrow \Re^1$

$$\mu(\vec{x}) = \mu(x,y,z) = \sum\sum\sum b_i^\mu(x) b_j^\mu(y) b_k^\mu(z) w_{ijk}^\mu. \tag{3}$$

Each attenuation coefficient μ is modelled as the product of several basis functions. With this representation the problem of finding μ has been transformed into the problem of estimating the parameters w^μ. The superscript μ is used to distinguish the attenuation parameters from deformation parameters.

3.2. The deformation model

The free form deformable model as presented by Rueckert [9] takes the same form as Eq. (3) but with the purpose of displacing voxels. The deformable model is based on a cubic spline and can be written as the function mapping $\varphi : \Re^3 \rightarrow \Re^3$ which takes in 3 coordinates (x,y,z) and outputs 3 transformed coordinates

$$(x',y',z') = (x,y,z) + (\triangle x, \triangle y, \triangle z) \tag{4}$$

$$\triangle x = \sum\sum\sum b_i^\varphi(x) b_j^\varphi(y) b_k^\varphi(z) w_{ijk}^\varphi. \tag{5}$$

The displacement in Eq. (4) is only given for the x direction, however y and z take exactly the same spline form but obviously with different parameters.

3.3. Error model

To determine the parameters of the attenuation and deformation models, an optimality criteria is needed. The observed data p_i corresponds to photon count data which leads to the reasonably assumption that they can be modelled as Poisson distributed random variables. Thus, we apply the likelihood function for Poisson statistics for computing similarity between observed and simulated data and hereby driving the estimation of the attenuation and deformation parameters, i.e.(assuming $r_i = 0$)

$$d(p_i, E[P_i]) = p_i \cdot \ln(E[P_i]) - E[P_i]. \tag{6}$$

Optimization of Eq. 2 requires the derivative of the cost function with respect to both the attenuation and motion parameters. These are found using the generalized chain rule. Let $l = \int_{L_i(\varphi)} \mu(\vec{x}) \partial\vec{x}$, then the derivatives are

Derivative with respect to attenuation

$$\frac{\partial C}{\partial w_{ijk}^\mu} = \sum_{i=1}^{N_p} (1 - \frac{P_i}{b_i e^{-l}}) b_i \cdot e^{-l} \cdot b_i^\mu(x) b_j^\mu(y) b_k^\mu(z), \tag{7}$$

Derivative with respect to motion

$$\frac{\partial C}{\partial w_{ijk}^\varphi} = \sum_{i=1}^{N_p} (1 - \frac{P_i}{b_i e^{-l}}) b_i \cdot e^{-l} \cdot \frac{\partial \mu}{\partial \varphi} \cdot b_i^\varphi(x) b_j^\varphi(y) b_k^\varphi(z). \tag{8}$$

The terms look similar but one notices that the first derivative expression only involves basis functions of the image attenuation model while the second includes the the spatial derivatives $\partial\mu/\partial\varphi$ of the image function and the basis functions of the deformation model.

3.4. Implementation details

We solve Eq. 2 by negating the cost function and derivatives and applying an L-BFGS-B minimization routine. Estimation of the two models is performed by two separate minimizations within the outer while loop. This essentially fixes one model while the other is being optimized. The procedure is outlined below,

1. Obtain start guess for attenuation
2. while (not converged)
   (a) Optimize C as function of the deformation model parameters.
   (b) Optimize C as a function of the attenuation model parameters.

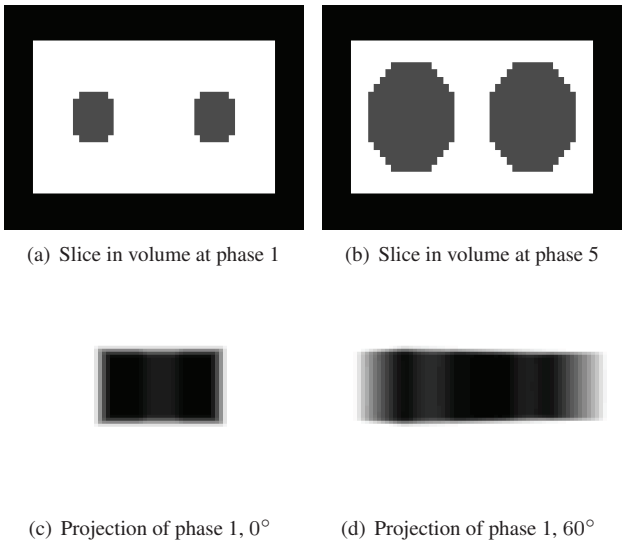

(a) Slice in volume at phase 1 (b) Slice in volume at phase 5

(c) Projection of phase 1, 0° (d) Projection of phase 1, 60°

Fig. 1. Shows phantom data and simulated projections. In the projections a dark pixel means high attenuation

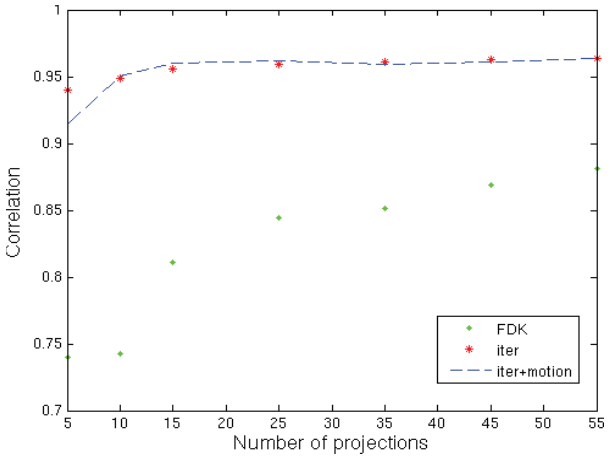

Fig. 2. Shows the cross correlation between reconstructions and the true volume for 7 experiments with a decreasing number of projections, using three different types of methods.

An advantage of using an L-BFGS-B is that it allows for bound constrained optimization which is used when estimating the attenuation coefficients, since by definition these are non-negative, however the bound constraint have no influence on the deformation model. The start guess came from the pure iterative method and the deformation model starts out with the identity transformation.

4. EXPERIMENTS

4.1. Cone-beam data

The data used for experimentation is based on simulated cone-beam projections. The benefit of doing this is twofold. First the knowledge of ground truth data may be useful for method validation, second noise and scattering problems are avoided. The projections are made from a phantom emulating 5 respiratory phases where each phase volume has two cylinders shaped objects that dilate with the phase number, hereby simulating motion. The point source and 2D detector are moved around the volume and a set of phase varying projections are made using the forward projection model of Eq. 2. The projection angle distribution was chosen at random. The detector was chosen to be 85×85 with a SDD of 200 mm and SAD of 150 mm.

An illustration of the raw data at phase 1 and 5, as well as simulated projections are shown in Fig 1.

4.2. Results

Seven reconstruction experiments were conducted to investigate the three methods of FDK with hamming filter, the iterative method and the iterative method with motion. These experiments are aimed at reconstructing phase 5 as shown in Fig 1(b). The base number of projections for each experiments is 55, 45, 35, 25, 15, 10 and 5. Since there are 5 phases, the reconstruction experiments with motion uses five times the number of projections. To compare the methods, we estimate the cross correlation between the ground truth and the estimated reconstructions.

A plot of the correlations for the seven test cases is shown in Fig. 2. It shows the lowest reconstruction error using the iterative method and (iterative + motion), however the difference is small and the results favour the iterative method since it use 5 times less projections.

Fig. 3 shows the same slice reconstructed using 55 and 10 projections with each of the three methods. These examples confirm what was observed from the error plot. At 5 projections the problem is highly under-constrained and the methods fail at supplying a satisfying solution. At 10 projections, the 2 iterative methods are becoming acceptable although they still show some artefacts. Even using 55 projections with FDK, the iterative solutions using only 10 projection looks visually more appealing emphasizing iterative methods ability to reconstruct using a low number of projections.

An important feature of the method including motion is the availability of the motion field which in the context of patient scenario could be used to track tumours across respiratory phases. No prior model assumption have been made about the deformation field but we are currently trying to find the most optimal choice and expect this will improve the results in favour of the iterative method with motion compensation.

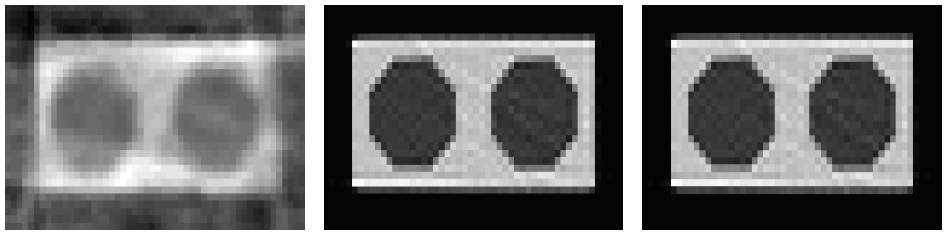

(a) FDK, 55 projections (b) Iterative, 55 projections (c) Iterative+motion, 55 projections

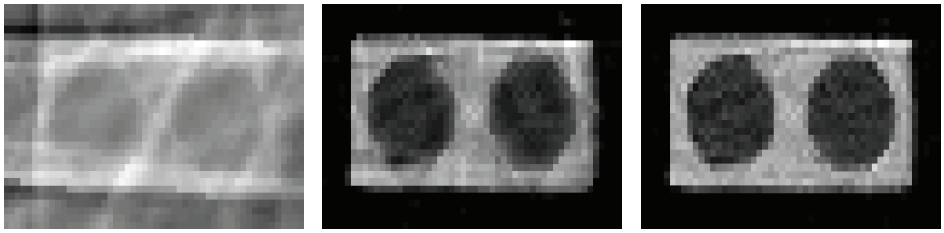

(d) FDK, 10 projections (e) Iterative, 10 projections (f) Iterative+motion, 10 projections

Fig. 3. Shows reconstruction experiments for tree different methods.

5. CONCLUSION

We have investigated the possibility of including a parametric motion model into a maximum likelihood reconstruction framework. Reconstruction errors with a known ground truth volume showed that the method clearly outperformed the FDK approach and in general performed similar to the pure iterative method. We believe the main reason for this results is the ill possessedness of the optimization problem requiring additional prior information to obtain a reasonable motion model. Inclusion of the best motion for constraining the problem is currently being investigated. In addition it is also being examined how the method could be accelerated through multi resolution schemes and the inclusion of mask containing information about object placements. Using such mask could speed up the runtime by limiting the regions over which to integrate lines.

6. REFERENCES

[1] L. A. Feldkamp, L. C. Davis, and J. W. Kress, "Practical cone-beam algorithm," *J. Opt. Soc. Am. A*, vol. 1, no. 6, pp. 612–619, June 1984.

[2] Ehrhardt J., Werner R., Frenzel T. Säring D., Low D. Lu W., and Handels H., "Reconstruction of 4D-CT data sets acquired during free breathing for the analysis of respiratory motion," march 2006, vol. 6144 of *Society of Photo-Optical Instrumentation Engineers (SPIE) Conference Series*, pp. 365–372.

[3] T Li, E Schreibmann, Y Yang, and L Xing, "Motion correction for improved target localization with on-board cone-beam computed tomography," *Physics in Medicine and Biology*, vol. 51, no. 2, pp. 253–267, 2006.

[4] Simon Rit, Jochem Wolthaus, Marcel Herk, and Jan-Jakob Sonke, "On-the-fly motion-compensated cone-beam ct using an a priori motion model," in *MICCAI '08: Proceedings of the 11th international conference on Medical Image Computing and Computer-Assisted Intervention - Part I*, Berlin, Heidelberg, 2008, pp. 729–736, Springer-Verlag.

[5] Chong Zhang, Mathieu De Craene, Maria-Cruz Villa-Uriol, and Alejandro F.Frangi Jose M.Pozo, Bart H. Bijnens, "Estimating continuous 4d wall motion of cerebral aneurysms from 3d rotational angiography," in *MICCAI 09: Proceedings of the 12th international conference on Medical Image Computing and Computer-Assisted Intervention*, September.

[6] Rongping Zeng, J.A. Fessler, and J.M. Balter, "Estimating 3-d respiratory motion from orbiting views by tomographic image registration," *IEEE Transactions on Medical Imaging*, vol. 26, no. 2, pp. 153–163, February 2007.

[7] Peihuang Lu, Jorge Nocedal, Ciyou Zhu, Richard H. Byrd, and Richard H. Byrd, "A limited-memory algorithm for bound constrained optimization," *SIAM Journal on Scientific Computing*, vol. 16, pp. 1190–1208, 1994.

[8] J. M. Fitzpatrick and M. Sonka, *"Handbook of Medical Imaging, Volume 2. Medical Image Processing and Analysis (SPIE Press Monograph Vol. PM80)"*, SPIE–The International Society for Optical Engineering, 1 edition, June 2000.

[9] D. Rueckert, L. Sonoda, I. Hayes, D. Hill, M. Leach, and D. Hawkes, "Nonrigid registration using free-form deformations: application to breast MR images.," *IEEE Trans Med Imaging*, vol. 18, no. 8, pp. 712–721, August 1999.